Statistical Mechanics of Semiflexible Bundles of Wormlike Polymer Chains

Claus Heussinger, Mark Bathe, and Erwin Frey

Arnold Sommerfeld Center for Theoretical Physics and CeNS, Department of Physics, Ludwig-Maximilians-Universität München, Theresienstrasse 37, D-80333 München, Germany

(Received 13 February 2007; published 25 July 2007)

We demonstrate that a semiflexible bundle of wormlike chains exhibits a state-dependent bending stiffness that alters fundamentally its scaling behavior with respect to the standard wormlike chain. We explore the equilibrium conformational and mechanical behavior of wormlike bundles in isolation, in cross-linked networks, and in solution.

DOI: 10.1103/PhysRevLett.99.048101 PACS numbers: 87.16.Ka, 82.35.Lr, 83.10.−y, 87.15.La

In recent decades, the wormlike chain (WLC) has emerged as the standard model for the description of semiflexible polymers [1]. The defining property of a WLC is a mechanical bending stiffness κ_f that is an intrinsic material constant of the polymer. Within this framework, numerous correlation and response functions have been calculated, providing a comprehensive picture of the equilibrium and dynamical properties of WLCs [2–4]. A number of experimental studies have demonstrated the applicability of the WLC model to DNA [5] and F-actin [6], among other biological and synthetic polymers. Significant progress has also been made towards the description of the collective properties of WLCs, for example, in the form of entangled solutions. One of the hallmarks of this development is the scaling of the plateau shear modulus with concentration $G \sim c^{7/5}$ [7–9], which is well established experimentally [10,11].

Another important emerging class of semiflexible polymers consists of *bundles* of WLCs [12,13]. Semiflexible polymer bundles consisting of F-actin or microtubules are ubiquitous in biology [14] and have unique mechanical properties that may well be exploited in the design of nanomaterials [13]. As shown by Bathe *et al.* [15,16], wormlike bundles (WLBs) have a state-dependent bending stiffness κ_B that derives from a generic interplay between the high stiffness of individual filaments and their rather soft relative sliding motion. In this Letter, we demonstrate that this state dependence gives rise to fundamentally new behavior that cannot be reproduced trivially using existing relations for WLCs. We explore the consequences of a state-dependent bending stiffness on the statistical mechanics of isolated WLBs, as well as on the scaling behavior of their entangled solutions and cross-linked networks.

We consider the bending of ordered bundles with an isotropic cross section. A bundle consists of N filaments of length L and bending stiffness κ_f. Filaments are irreversibly cross-linked to their nearest neighbors by discrete cross-links with mean axial spacing δ. Cross-links are modeled to be compliant in shear along the bundle axis with finite shear stiffness $k_\times$ and to be inextensible transverse to the bundle axis, thus fixing the interfilament distance b [17]. Bundle deformations are characterized by the transverse deflection $\mathbf{r}_\perp(s)$ of the bundle neutral surface at axial position s along the backbone and by the stretching deformation $u_i(s)$ of filament i. The torsional stiffness of the bundle is assumed to be of the same order as the bending stiffness. Thus, as long as transverse deflections remain small ("weakly bending"), the two components of $\mathbf{r}_\perp$ are decoupled, and the effects of twist are of higher order [18]. The bundle response may then be analyzed in planar deformation, where the bending stiffness results from the superposition of $2M = \sqrt{N}$ bundle layers.

The WLB Hamiltonian consists of three contributions $H_{\mathrm{WLB}} = H_{\mathrm{bend}} + H_{\mathrm{stretch}} + H_{\mathrm{shear}}$. The first term corresponds to the standard WLC Hamiltonian

$$H_{\mathrm{bend}} = \frac{N\kappa_f}{2} \int_0^L ds \left(\frac{\partial^2 r_\perp}{\partial s^2}\right)^2, \tag{1}$$

which is the same for each of the N filaments. The second term accounts for filament stretching

$$H_{\mathrm{stretch}} = Mk_s\delta \int_0^L ds \sum_{i=-M}^{M-1} \left(\frac{\partial u_i}{\partial s}\right)^2, \tag{2}$$

where k_s is the single filament stretching stiffness on the scale of the cross-link spacing δ. No particular form for bending and stretching stiffnesses is assumed, but one may think of the filaments as homogeneous elastic beams with Young's modulus E, for which $\kappa_f \sim Eb^4$ and $k_s \sim Eb^2/\delta$. Alternatively, k_s may represent the entropic elasticity of a WLC, for which $k_s \sim \kappa_f^2/T\delta^4$.

The third energy contribution H_{shear} results from the cross-link-induced coupling of neighboring filaments. To minimize the cross-link energy, any relative filament slip induced by cross-sectional rotations $\theta = \partial_s r_\perp \equiv r'_\perp$ must be compensated by filament stretching (Fig. 1). This cross-link shear energy, which simply suppresses relative sliding motion of neighboring filaments, is given by

$$H_{\mathrm{shear}} = \frac{Mk_\times}{\delta} \int_0^L ds \sum_{i=-M+1}^{M-1} \left(\Delta u_i + b\frac{\partial r_\perp}{\partial s}\right)^2, \tag{3}$$

where $\Delta u_i = u_i - u_{i-1}$. A related model for two filaments was introduced by Everaers, Bundschuh, and Kremer in

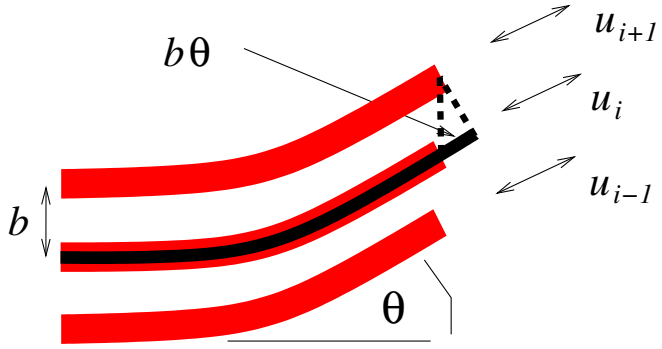

FIG. 1 (color online). Illustration of the geometry of a single bundle layer (the full bundle consists of $2M$ layers that are stacked in parallel). The bundle is deflected through the angle $\theta = r'_\perp$. If filament i stretches the amount $u_i = u_{i+1} + b\theta$, the cross-link (dashed line) remains undeformed with zero shear energy.

Ref. [19], where special emphasis was placed on the limit of inextensible filaments $k_s \to \infty$. In that model, the anisotropic bundle cross section leads to a coupling of in-plane and out-of-plane bending modes [20] that is absent in the present model because it has a symmetric cross section.

Functional differentiation of the Hamiltonian results in the (overdamped) equations of motion

$$N\kappa_f r''''_\perp - \frac{2Mk_\times b}{\delta}\sum_i (\Delta u'_i + b r''_\perp) = F(r_\perp, s), \qquad (4)$$

$$k_s \delta u''_i + \frac{k_\times}{\delta}(\Delta u_{i+1} - \Delta u_i) = 0, \qquad (5)$$

where F is a transverse force that may represent fluid drag, random thermal noise, or other external loading. To proceed, Eq. (5) is solved together with appropriate boundary conditions, so as to eliminate the u_i in Eq. (4). The calculations are most easily performed in Fourier space, where we write for the expansions $r_\perp(s) = \sum_n r_n \sin(n\pi s/L)$ and $u_i(s) = \sum_n u_{in} \cos(n\pi s/L)$, applicable to pinned boundary conditions. The resulting equation of motion for r_n then takes the simple form $\kappa_n q_n^4 r_n = F_n$, with a mode-number-dependent effective bending stiffness κ_n. The general result for κ_n is obtained using the standard ansatz $u_i \sim w^i$, which reduces Eq. (5) to an equation that is quadratic in w.

In the following, we present an approximate solution to Eqs. (4) and (5) that is based on the assumption that filament stretching increases *linearly* through the bundle cross section $u_i = \Delta u(i + 1/2)$ [21]. Although comparison with the exact solution demonstrates that u_i, in general, varies nonlinearly with i [22], it turns out that the effective bending stiffness κ_n is insensitive to this nonlinearity. At the same time, the linearization simplifies the formulas substantially, so that the effective bending stiffness is given in closed form by

$$\kappa_n = N\kappa_f\left[1 + \left(\frac{12\hat{\kappa}_f}{N-1} + (q_n\lambda)^2\right)^{-1}\right], \qquad (6)$$

with a dimensionless bending stiffness $\hat{\kappa}_f = \kappa_f/k_s\delta b^2$ and a length scale $\lambda = (L/\sqrt{\alpha})\sqrt{M\hat{\kappa}_f/(M - 1/2)}$ that depends on the shear stiffness $k_\times$ via the dimensionless coupling parameter $\alpha = k_\times L^2/k_s\delta^2$.

For any given mode number $q_n \sim n/L$, three different elastic regimes emerge as asymptotic solutions for $N \gg 1$ and respective values of α [15,16]. For large shear stiffness ($\alpha \gg N$), the *fully coupled* bending scenario is obtained, where the bundle behaves like a homogeneous beam with $\kappa_n \sim N^2 k_s$. For intermediate values of the shear stiffness ($1 \ll \alpha \ll N$), the bending stiffness in the *shear-dominated* regime is $\kappa_n \sim Nk_\times q_n^{-2}$ and the full mode-number dependence of Eq. (6) has to be accounted for. Finally, *decoupled bending* of N laterally independent, but transversely constrained, filaments is found in the limit of small cross-link shear stiffness ($\alpha \ll 1$), where the bending stiffness is simply $\kappa_n = N\kappa_f$.

In the particular limit of $N \to \infty$ and fixed bundle diameter $D = b\sqrt{N} \ll L$, Eq. (6) reduces to the Timoshenko model for beam bending [23], which was recently used to interpret bending stiffness measurements on microtubules [24,25] and carbon nanotube bundles [13]. In this limit,

$$\kappa_n = \frac{N^2\kappa_f}{1 + (q_n D)^2 E/12G}, \qquad (7)$$

where we have used the expressions of k_s and κ_f for homogeneous beams and defined $G = k_\times/\delta$. While this limit serves as a consistency check for our mathematical analysis, real bundles consist of a finite, and often small, number of constituent filaments, for which Eq. (7) cannot be applied to describe the full range of bending behavior captured by Eq. (6). Indeed, in Eq. (7), no decoupled bending regime exists, and the bending stiffness vanishes as the cross-link shear stiffness approaches zero [26]. The condition $\alpha \sim N$ delineating the remaining two regimes can be rewritten as $E/G \sim (L/D)^2 \gg 1$, which reemphasizes the small value of cross-link shear stiffness in the intermediate regime.

For fixed values of (N, α), the bundle bending stiffness Eq. (6) crosses over from fully coupled to decoupled bending via the intermediate regime as the mode number q_n is increased. Thus, different modes may belong to different elastic regimes, rendering the fluctuation properties of the bundle nontrivial and qualitatively different from single semiflexible polymers. This crossover is mediated by the length scale λ, which acts as a cutoff on the fluctuation spectrum: Whereas wavelengths $q_n^{-1} \ll \lambda$ belonging to the decoupled regime are characterized by a constant bending stiffness, modes with $q_n^{-1} \gg \lambda$ acquire a higher stiffness $\kappa_n \sim q_n^{-2}$ and are thereby suppressed. Finally, for even longer wavelengths $q_n^{-1} \gg \lambda\sqrt{N}$, the bending stiffness reattains a constant, limiting value. As an example (taken from Ref. [12]), we found $\lambda \approx 7\ \mu$m for actin/fascin bundles with $N \approx 30$, $L \approx 50\ \mu$m.

In situations where modes pertaining to the intermediate regime are irrelevant, the q dependence of κ_n drops out, and one recovers the single WLC result, albeit with a renormalized persistence length $l_p \to N l_p$ in the decoupled and $l_p \to N^2 l_p$ in the fully coupled regimes, respectively. In other cases, calculation of the tangent-tangent correlation function demonstrates that the persistence length cannot be defined unambiguously. As indicated in Ref. [19], the correlation function does not decay exponentially but rather exhibits a complex structure at intermediate distances [22]. In the following, we will therefore explore the consequences on the statistical mechanics of the WLB, in particular, as regards the intermediate regime.

First, consider the force-extension relation as calculated from the end-to-end distance $R(F) = L - \sum_n k_B T/(\kappa_n q_n^2 + F)$, where F is the force applied to the bundle ends [27]. For small stretching forces, one may readily calculate the linear response coefficient $k_{\text{entr}} = F/[R(F) - R(0)]$ using a Taylor series expansion. The result in the intermediate regime is

$$k_{\text{entr}} \propto \frac{(N\kappa_f)^2}{L\lambda^3 k_B T} \quad (\lambda\sqrt{N} \gg L \gg \lambda), \tag{8}$$

which is inversely proportional to bundle length, like a mechanical beam. Importantly, the strong dependence of $k_{\text{entr}}(L) \sim L^{-4}$ applicable to single filaments (and the other two regimes) is lost. This has dramatic consequences on the plateau value of the shear modulus G in cross-linked bundle networks, which in affine theories [28] is assumed to be given in terms of k_{entr} by $G \sim k_{\text{entr}}(\xi)/\xi$, where the mesh size ξ depends on concentration c as $\xi \sim c^{-1/2}$. Accordingly, in the intermediate regime one finds $G \sim c$, which is a much weaker concentration dependence than $G \sim c^{5/2}$ [29] applicable to single filaments. It is worthwhile noting that the force-extension relation is strongly nonlinear (see Fig. 2), rendering the linear response valid only for very small relative extensions. In this particular example, the linear response formula deviates from the exact solution by 50% at only $\approx 3\%$ and $\approx 0.7\%$ strain in the decoupled and the fully coupled limits, respectively.

Bundle behavior under compressive forces further highlights the unusual properties of WLBs. Because the bending stiffness in the intermediate regime scales with the length of the bundle as $\kappa_B \sim L^2$, the Euler buckling force $F_c \sim \kappa_B/L^2 \sim N\kappa_f/\lambda^2$ is *independent* of bundle length. This unique property may well be exploited in polymerizing biological bundles such as filopodia, which may increase their contour length against compressive loads without loss of mechanical stability.

Complementary to the elasticity of cross-linked networks of WLBs, we turn next to the elasticity of their entangled solutions. The generally accepted theory for the concentration dependence of the plateau modulus of entangled WLCs is based on the free energy change ΔF of confining a polymer to a tube of diameter d [7,8]. The

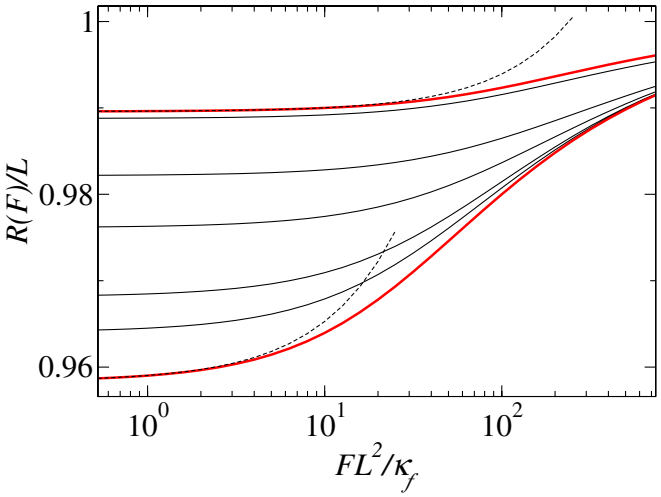

FIG. 2 (color online). End-to-end distance $R(F)/L$ as a function of stretching force FL^2/κ_f for a bundle of $N = 4$ filaments and $L = l_p$. The black curves correspond to $\lambda/L = 0.01, 0.1, \ldots, 0.7$. The thick (red) curves relate to (bottom) decoupled and (top) fully coupled bending, respectively. The dashed lines correspond to the respective linear response regimes.

associated change in free energy is written as $\Delta F \sim k_B T L/l_d$, which defines the deflection length l_d to be the scale at which the polymer starts to interact with its enclosing tube. The deflection length itself is connected to the tube diameter d and the filament concentration c via the standard excluded volume argument [9] $l_d^2 d = l_d/cL$, which balances the excluded volume of the tube with the available volume per filament. All that remains is the calculation of the tube diameter d of a single polymer confined by the potential

$$V = \frac{N\kappa_f}{2l_c^4} \int_0^L ds r_\perp^2(s), \tag{9}$$

where the confinement length l_c is defined as a measure of the strength of the potential. While $l_c \equiv l_d$ in the standard WLC, we will see shortly that this does not hold for WLBs in the intermediate regime. First, consider the transverse fluctuations of an unconfined bundle, in particular, the average value $d_0^2 \equiv \frac{1}{L}\int_s \langle r_\perp(s)^2 \rangle$. This is most easily calculated as

$$d_0^2 \sim L\lambda^2/N l_p \quad (\lambda\sqrt{N} \gg L \gg \lambda), \tag{10}$$

which has to be compared to the WLC result for which $d_0^2 \sim L^3/l_p$. In the presence of the confining potential, the same calculation yields

$$d^2 \sim l_c^2 \lambda/N l_p \quad (\lambda\sqrt{N} \gg l_c \gg \lambda). \tag{11}$$

For strong confinement $l_c \ll \lambda$, the potential suppresses all modes of the intermediate regime, and one recovers the expression valid for single filaments: $d^2 \sim l_c^3/l_p$. The general result for the tube diameter is depicted in Fig. 3. As the

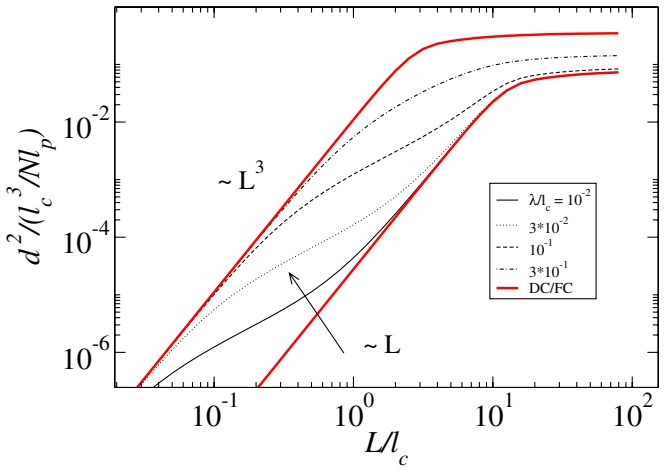

FIG. 3 (color online). Tube diameter $d^2/(l_c^3/Nl_p)$ as a function of contour length L/l_c for various λ/l_c and $M = 20$. Thick (red) curves correspond to (top) decoupled and (bottom) fully coupled bending, respectively. For short filaments, the intermediate regime is visible through the linear slope $d^2 \sim L$ [see Eq. (10)]. For long filaments, the fluctuations saturate. By increasing λ, the tube is becoming wider [Eq. (11)].

contour length L of the bundle is increased, it begins to ''feel'' the presence of its enclosing tube at the deflection length $L = l_d$. By comparing Eq. (10) with Eq. (11), one finds $l_d \sim l_c^2/\lambda$, which is valid in the intermediate regime. At the same time, $l_d \equiv l_c$ in the decoupled and fully coupled regimes, where the deflection and confinement lengths are identical.

One may use these results to rewrite the deflection length as a function of concentration c. In the intermediate regime, the result is $l_d^3 \sim Nl_p/(\lambda cL)^2$, which replaces the usual result $l_d^5 \sim Nl_p/(cL)^2$ valid in the decoupled regime (strong confinement). The free energy of confinement and the elastic plateau modulus $G \sim (cL)\Delta F/L$ now depend on λ and thus on the properties and density of the cross-links. The modulus displays a crossover that is *mediated by concentration*:

$$G \sim k_B T \begin{cases} (cL)^{5/3}(Nl_p)^{-1/3}\lambda^{2/3}, & c \ll c^\star, \\ (cL)^{7/5}(Nl_p)^{-1/5}, & c \gg c^\star, \end{cases} \qquad (12)$$

where we defined the crossover concentration as $(cL)^\star \sim \sqrt{Nl_p}\lambda^{-5/2}$. Below the even smaller concentration $c^{\star\star} \sim c^\star N^{-3/4}$, the fully coupled regime is entered, and the modulus again scales as $G \sim c^{7/5}$.

Having addressed equilibrium properties of WLBs, further consequences of the state-dependent bending stiffness on dynamic response functions remain to be explored, along with the effects of nonpermanent cross-links. Additional experiments [12,13,21,30] are required to test the applicability of the derived results to biological and synthetic bundles.

Funding from the Alexander von Humboldt Foundation (to M. B.), from the German Science Foundation (SFB 486), and from the German Excellence Initiative via the program ''Nanosystems Initiative Munich (NIM)'' is gratefully acknowledged.

[1] N. Saitô, K. Takahashi, and Y. Yunoki, J. Phys. Soc. Jpn. **22**, 219 (1967).
[2] R. Granek, J. Phys. II **7**, 1761 (1997).
[3] J. F. Marko and E. D. Siggia, Macromolecules **28**, 8759 (1995).
[4] J. Wilhelm and E. Frey, Phys. Rev. Lett. **77**, 2581 (1996).
[5] C. Bustamante, J. F. Marko, E. D. Siggia, and S. Smith, Science **265**, 1599 (1994).
[6] L. Le Goff, O. Hallatschek, E. Frey, and F. Amblard, Phys. Rev. Lett. **89**, 258101 (2002).
[7] H. Isambert and A. C. Maggs, Macromolecules **29**, 1036 (1996).
[8] T. Odjik, Macromolecules **16**, 1340 (1983).
[9] A. N. Semenov, J. Chem. Soc., Faraday Trans. 2 **82**, 317 (1986).
[10] B. Hinner *et al.*, Phys. Rev. Lett. **81**, 2614 (1998).
[11] J. Xu, A. Palmer, and D. Wirtz, Macromolecules **31**, 6486 (1998).
[12] M. M. A. E. Claessens, M. Bathe, E. Frey, and A. R. Bausch, Nat. Mater. **5**, 748 (2006).
[13] A. Kis *et al.*, Nat. Mater. **3**, 153 (2004).
[14] H. Lodish *et al.*, *Molecular Cell Biology* (Palgrave Macmillan, London, 2003), 5th ed.
[15] M. Bathe, C. Heussinger, M. Claessens, A. Bausch, and E. Frey, arXiv:q-bio.BM/0607040.
[16] M. Bathe, C. Heussinger, M. Claessens, A. Bausch, and E. Frey (to be published).
[17] Typical protein elongational stiffnesses are of the order 1 N/m, while they are much softer in shear [12].
[18] L. D. Landau and E. M. Lifshitz, *Theory of Elasticity* (Butterworth-Heinemann, Oxford, 1995), Vol. 7, 3rd ed.
[19] R. Everaers, R. Bundschuh, and K. Kremer, Europhys. Lett. **29**, 263 (1995).
[20] B. Mergell, M. R. Ejtehadi, and R. Everaers, Phys. Rev. E **66**, 011903 (2002).
[21] J. A. Tolomeo and M. C. Holley, Biophys. J. **73**, 2241 (1997).
[22] C. Heussinger *et al.* (to be published).
[23] J. M. Gere and S. P. Timoshenko, *Mechanics of Materials* (Nelson Thornes Ltd., Cheltenham, 2002), 5th ed.
[24] F. Pampaloni *et al.*, Proc. Natl. Acad. Sci. U.S.A. **103**, 10 248 (2006).
[25] A. Kis *et al.*, Phys. Rev. Lett. **89**, 248101 (2002).
[26] Reanalyzing the data of [24], we expect microtubules shorter than $L \approx 3.5$ μm to be in the decoupled regime with a constant persistence length $l_p \approx 0.18$ mm.
[27] Note that a second contribution from the extensibility of the bundle backbone is neglected here for simplicity.
[28] M. Rubinstein and R. H. Colby, *Polymer Physics* (Oxford University Press, New York, 2003).
[29] F. C. MacKintosh, J. Käs, and P. A. Janmey, Phys. Rev. Lett. **75**, 4425 (1995).
[30] O. Lieleg *et al.*, arXiv:cond-mat/0611752.